



HAL
open science

Characteristics of colored dissolved organic matter (CDOM) in the Western Arctic Ocean: relationships with microbial activities

Atsushi Matsuoka, Eva Ortega-Retuerta, Annick Bricaud, Kevin R Arrigo, Marcel Babin

► To cite this version:

Atsushi Matsuoka, Eva Ortega-Retuerta, Annick Bricaud, Kevin R Arrigo, Marcel Babin. Characteristics of colored dissolved organic matter (CDOM) in the Western Arctic Ocean: relationships with microbial activities. *Deep Sea Research Part II: Topical Studies in Oceanography*, 2015, 118 (Part A), pp.44-52. 10.1016/j.dsr2.2015.02.012 . hal-01120307

HAL Id: hal-01120307

<https://hal.sorbonne-universite.fr/hal-01120307>

Submitted on 25 Feb 2015

HAL is a multi-disciplinary open access archive for the deposit and dissemination of scientific research documents, whether they are published or not. The documents may come from teaching and research institutions in France or abroad, or from public or private research centers.

L'archive ouverte pluridisciplinaire **HAL**, est destinée au dépôt et à la diffusion de documents scientifiques de niveau recherche, publiés ou non, émanant des établissements d'enseignement et de recherche français ou étrangers, des laboratoires publics ou privés.

1 **Characteristics of colored dissolved organic matter (CDOM) in the Western Arctic**

2 **Ocean: relationships with microbial activities**

3

4 Atsushi Matsuoka^{1,2,3*}

5 *Corresponding author

6

7 Affiliation 1: *Takuvik* Joint International Laboratory, Département de Biologie, Université Laval,

8 1045, avenue de la Médecine, Québec, QC, G1V 0A6, Canada

9 E-mail : Atsushi.Matsuoka@takuvik.ulaval.ca

10 Phone : +1 (418) 656 2131

11 Fax : +1 (418) 656 2339

12

13 Affiliation 2: *Takuvik* Joint International Laboratory, CNRS, 1045, avenue de la Médecine,

14 Québec, QC, G1V 0A6, Canada

15

16 Affiliation 3: Laboratoire d'Océanographie de Villefranche, Université Pierre et Marie Curie

17 (Paris 6)/CNRS, B.P. 8, Villefranche-sur-Mer Cedex, 06238, France

18

19 Eva Ortega-Retuerta^{1,2,3}

20 Affiliation 1: Dpt. Biologia Marina i Oceanografia, Institut de Ciències del Mar-CSIC, 08003

21 Barcelona, Spain

22 E-mail : ortegaretuerta@icm.csic.es

23 Phone : +34 93 230 96 06

24 Fax : +34 93 230 95 55

25

26 Affiliation 2: Sorbonne Universités, UPMC Paris 06, UMR 7621, Laboratoire d'Océanographie

27 Microbienne, Observatoire Océanologique, F-66650 Banyuls/mer, France

28

29 Affiliation 3 : CNRS, UMR 7621, Laboratoire d'Océanographie Microbienne, Observatoire

30 Océanologique, F-66650 Banyuls-sur-mer, France

31

32 Annick Bricaud^{1,2}

33 Affiliation 1: Sorbonne Universités, UPMC Paris 06, UMR 7093, LOV, Observatoire

34 Océanographique, F-06230 Villefranche/mer, France

35 E-mail: annick@obs-vlfr.fr

36 Phone : +33 (0)4 93 76 37 13

37 Fax : +33 (0)4 93 76 37 39

38

39 Affiliation 2: CNRS, UMR 7093, LOV, Observatoire Océanographique, F-06230

40 Villefranche/mer, France

41

42 Kevin R. Arrigo

43 Affiliation: Department of Environmental Earth System Science, Stanford University, Stanford,

44 California, 94305, USA

45 E-mail : arrigo@stanford.edu

46 Phone : +1 (650) 723 3599

47 Fax : +1 (650) 498 5099

48

49 Marcel Babin^{1,2,3}

50 Affiliation 1: *Takuvik* Joint International Laboratory, Département de Biologie, Université Laval,

51 1045, avenue de la Médecine, Québec, QC, G1V 0A6, Canada

52 E-mail : Marcel.Babin@takuvik.ulaval.ca

53 Phone : +1 (418) 656 2131

54 Fax : +1 (418) 656 2339

55

56 Affiliation 2: *Takuvik* Joint International Laboratory, CNRS, 1045, avenue de la Médecine,

57 Québec, QC, G1V 0A6, Canada

58

59 Affiliation 3: Laboratoire d'Océanographie de Villefranche, Université Pierre et Marie

60 Curie(Paris 6)/CNRS, B.P. 8, Villefranche-sur-Mer Cedex, 06238, France

61

62 **Abstract**

63 Colored dissolved organic matter (CDOM), a significant fraction of dissolved organic carbon
64 (DOC), plays various roles in physical and biogeochemical processes in natural waters. In the Arctic
65 Ocean, CDOM is abundant because of major input by large rivers. To better understand the
66 processes that drive variations in CDOM, light absorption coefficients of CDOM [$a_{\text{CDOM}}(\lambda)$, m^{-1}]
67 were extensively documented together with temperature, salinity, chlorophyll *a*, nitrate
68 concentrations, and bacterial production (BP) and abundance (BA) in the Western Arctic Ocean
69 (WAO) from early to late summer as part of the MALINA and the ICESCAPE expeditions. The
70 data set covered contrasting situations, from bloom to post-bloom conditions and from river-
71 influenced to oceanic water masses. While CDOM photobleaching occurred in the surface layer (<
72 20 m), we observed significantly lower spectral slopes for CDOM absorption spectra (S_{CDOM}) in
73 addition to higher $a_{\text{CDOM}}(440)$ in the layer below (intermediate layer: $30.7 < \text{salinity} < 33.9$). In
74 particular, the low S_{CDOM} values were found in the Chukchi Sea and the western part of the Beaufort
75 Sea, which coincided with high BP and BA values. Considering the high primary production
76 observed in these areas during our cruises (Arrigo et al., 2012), we hypothesize that S_{CDOM}
77 variations reflect the degradation of phytoplankton that is associated with heterotrophic bacterial
78 activity. In our datasets, a simple regression analysis showed that S_{CDOM} was significantly correlated

79 with BP and BA. A principal component analysis further supported this conclusion. From our field
80 observations, it was shown that variations in $a_{CDOM}(440)$ and S_{CDOM} result to a large extent from
81 bacterial activity, at least in the WAO.

82 1. Introduction

83 Examining the budget of dissolved organic carbon (DOC) in the Arctic Ocean is crucial to
84 improving our understanding of modifications in the carbon cycle resulting from ongoing global
85 warming. While this warming likely induces thawing of permafrost containing a huge amount of
86 DOC, which is subsequently delivered by river discharge into the Arctic Ocean (Peterson et al.,
87 2002; McClelland et al., 2006; Raymond et al., 2007), the long-term trend in the DOC budget of the
88 Pan-Arctic Ocean has yet to be established. In recent studies, Matsuoka et al. (2013, 2014)
89 developed a semi-analytical algorithm to quantitatively estimate DOC concentrations for Arctic
90 coastal waters using satellite remote sensing data, which allows the continuous monitoring of
91 variability in DOC concentrations. In contrast, knowledge about the production and the removal
92 processes gained from field observations using traditional methods is limited temporally and
93 geographically (Bussmann, 1999; Garneau et al., 2008; Kirchman et al., 2009; Ortega-Retuerta et
94 al., 2012). This prevents us from understanding the balance between these processes.

95 Light absorption by the colored fraction of dissolved organic matter (CDOM) provides useful
96 information about biogeochemical processes (Carder et al., 1989; Nelson et al., 1998; Miller et al.,
97 2002; Nelson et al., 2004, 2007; Matsuoka et al., 2012). While microbial activity is highly variable
98 in natural environments (e.g., Azam et al., 1983), the link between heterotrophic bacterial
99 production and CDOM absorption was reported in the Sargasso Sea (Nelson et al., 1998). More
100 recently, Matsuoka et al. (2012) suggested that lower spectral slopes of CDOM absorption spectra
101 observed in some Arctic Ocean water masses resulted from heterotrophic microbial activity.
102 However, a direct relationship between CDOM and bacteria has not been well documented.

103 The objective of this study is to examine the relationships between CDOM absorption properties
104 and heterotrophic bacterial production (BP) and abundance (BA) in the Western Arctic Ocean

105 (WAO) as well as their link with environmental variables (i.e., temperature, salinity, and nitrate and
106 chlorophyll *a* concentrations).

107

108 **2. Datasets and methods**

109 Data were collected during three cruises in the WAO (Figure 1): the joint France-Canada-USA
110 Arctic campaign, MALINA (30 July to 27 August 2009), and the National Aeronautics and Space
111 Administration (NASA) ICESCAPE cruises in 2010 and 2011 (referred to as ICESCAPE 2010: 15
112 June to 22 July 2010 and ICESCAPE 2011: 25 June to 29 July 2011, respectively). While waters in
113 the Mackenzie shelf-basin area during the MALINA cruise were oligotrophic and typical of post-
114 bloom conditions (Ortega-Retuerta et al., 2012), waters in the Chukchi-Beaufort Seas during the
115 ICESCAPE cruises were highly productive (Arrigo et al., 2012). To examine the general
116 characteristics in the WAO, these three datasets were combined and used in this study.

117 Temperature and salinity profiles were obtained using a SBE-911 plus (Seabird) conductivity-
118 temperature-depth (CTD) probe. Chlorophyll *a* (chl *a*) and phaeopigment concentrations (mg m^{-3})
119 were determined fluorometrically (Holm-Hansen et al., 1965). Nitrate concentrations (NO_3 , μmol
120 kg^{-1}) were measured following Grasshoff et al. (1999) for MALINA and Armstrong et al. (1967) for
121 ICESCAPE cruises. Oxygen concentrations (Oxy , $\mu\text{mol kg}^{-1}$) were measured following Carpenter
122 (1965) with modifications by Culberson et al. (1991).

123 Apparent oxygen utilization (AOU, $\mu\text{mol kg}^{-1}$) was calculated by referring solubility of oxygen
124 for well-mixed winter waters having temperature and salinity of -1.8°C and 31, respectively. These
125 reference data were proven to be valid for western Arctic waters (Matsuoka et al., 2012).

126

127 **2.1. CDOM absorption**

128 Details of the method used for measurement of CDOM absorption are documented in Matsuoka
129 et al. (2012). Briefly, water samples were filtered using $0.2\ \mu\text{m}$ pore-size filters immediately after
130 sampling. Absorption coefficients of CDOM ($a_{\text{CDOM}}(\lambda)$, m^{-1}) were determined from 200 to 735 nm

131 in 1-nm increments using a liquid waveguide system (UltraPath, World Precision Instruments, Inc.).
132 The spectral slope of $a_{\text{CDOM}}(\lambda)$ (S_{CDOM} , nm^{-1}) was calculated by nonlinear regression of the data
133 from 350 to 500 nm (Babin et al., 2003; Matsuoka et al., 2011, 2012).

134 A previous study (Helms et al., 2008) showed that the spectral slopes ($S_{275-295}$ and $S_{350-400}$, nm^{-1}
135 for both) corresponding to two distinct wavelength ranges (i.e., 275-295 nm and 350-400 nm,
136 respectively) and their ratio (S_R , dimensionless) provide insights into sources (e.g., marine or
137 terrestrial sources; Carder et al., 1989; Nelson et al., 2007) and/or local processes affecting the
138 CDOM distribution (e.g., lateral transport, vertical mixing, photo-bleaching, heterotrophic bacterial
139 alteration; Nelson et al., 1998, 2004; Matsuoka et al., 2012; Yamashita et al., 2013). These slope
140 parameters were calculated for our Arctic datasets by fitting a linear model to CDOM absorption
141 coefficients in the two distinct spectral ranges (Helms et al., 2008).

142

143 2.2. Bacterial abundance

144 Heterotrophic prokaryotes, including bacteria and archaea, are abbreviated throughout the
145 manuscript as “bacteria”. Samples were fixed with glutaraldehyde (0.25% final concentration) and
146 stored at -80°C until processing. During MALINA, bacterial cells (BA) were counted aboard the
147 ship by flow cytometry using a FACS ARIA (Becton, Dickinson and company) equipped with 488
148 nm and 633 nm lasers and a standard filter setup (Ortega-Retuerta et al., 2012). During ICESCAPE
149 2010, bacterial cells were counted by flow cytometry at the home laboratory using a BD FACS
150 Calibur Flow Cytometer (Becton, Dickinson and company). During ICESCAPE 2011, bacterial
151 cells were counted aboard the ship using an Accuri C6 (Becton, Dickinson and company) equipped
152 with a 488 nm laser. In all cases, samples were thawed and SYBR Green-I was added at a final
153 dilution of 1:10,000. Samples were incubated in the dark for 15 min before analysis. Bacterial cells
154 were identified on a plot of green fluorescence (515-545 nm) versus right angle light scatter (SSC),
155 using the green fluorescence as a threshold parameter. High nucleic acid (HNA) and low nucleic
156 acid (LNA) bacteria were discriminated according to their green fluorescence and counted

157 separately (Marie et al., 1997). HNA cells have often been considered as active bacteria (Gasol et al.,
158 1999).

159

160 2.3. Bacterial production

161 Bacterial production (BP) was measured following Ortega-Retuerta et al. (2012). Briefly BP was
162 measured by ^3H -leucine incorporation (Smith and Azam, 1992). Samples (1.5 mL in triplicate plus
163 one killed control) were added to sterile microcentrifuge tubes, containing 20-30 nM [4,5- ^3H]-
164 leucine. This concentration was sufficient to saturate bacterial leucine uptake (data not shown).
165 Incorporation rates were measured after 2-h incubations at *in situ* temperature, and incubations were
166 stopped by the addition of trichloroacetic acid (5% final concentration). Leucine incorporation rates
167 were converted to carbon production using the conversion factor of 1.5 kg C produced per mole of
168 leucine incorporated (Kirchman, 1993), considering no isotope dilution.

169

170 2.4. Statistical analyses

171 2.4.1. Regression analysis

172 To examine a direct relationship between two variables, several regression analyses were
173 performed. Because the two variables were random (or not controlled), Model II regression was
174 applied in this study (Legendre and Legendre, 1998).

175

176 2.4.2. Principal component analysis

177 For a dataset containing several variables, a multiple regression analysis is not always the best
178 method for examining the relationships among the variables. Principal component analysis (PCA) is
179 preferable because it summarizes, in a few dimensions, most of the variability present in a
180 dispersion matrix of a large number of variables (Legendre and Legendre, 1998), and has been
181 applied to a large number of oceanographic studies (e.g., Legendre and Legendre, 1998; Uitz et al.,
182 2008; Suzuki et al., 2012). We thus applied this method to our datasets.

183

184 2.5. Sea ice concentration

185 Daily sea ice concentrations data acquired by the Defense Meteorological Satellite Program
186 (DMSP) SSM/I passive microwave sensor (25-km spatial resolution) were downloaded from the
187 National Snow and Ice Data Center (NSIDC) at
188 ftp://sidacs.colorado.edu/pub/DATASETS/nsidc0051_gsfc_nasateam_seaice/. Daily images (29 for
189 MALINA, 38 for ICESCAPE2010, and 35 for ICESCAPE2011) were averaged to generate an
190 image of mean sea ice concentrations for each cruise (Figure 2).

191

192 **3. Results and discussion**193 **3.1. Vertical distribution of CDOM**

194 To examine the vertical distribution of CDOM absorption properties in the WAO, $a_{\text{CDOM}(440)}$
195 and S_{CDOM} were plotted against depth (Figure 3). At depth < 150 m, $a_{\text{CDOM}(440)}$ values were highly
196 variable for early to middle summer (ICESCAPE2010 and 2011 data: blue crosses and red
197 diamonds in Figure 3a and c). Values for late summer (MALINA data: black circles in Figure 3a),
198 however, were less variable and low near the surface (down to 0.0197 m^{-1}), except for river waters
199 that showed significantly higher values (up to 1.08 m^{-1} ; see arrow in Figure 3a). At depth > 150 m,
200 all data tended to decrease with depth, approaching $0.0277 \pm 0.0025 \text{ m}^{-1}$ (dotted rectangle in Figure
201 3c). This type of profile was similar to that reported by Guéguen et al. (2012), who suggested that
202 the maximal values around 150 m are associated with microbial activity (see sections 3.3 and 3.4).
203 While determination of the origin of CDOM (e.g., production by phytoplankton, heterotrophic
204 bacteria, etc) is still challenging using our dataset alone, we acknowledge that phytoplankton
205 especially at the deep chlorophyll maximum is one of the CDOM sources (Matsuoka et al, 2012).

206 Similarly to $a_{\text{CDOM}(440)}$, S_{CDOM} values for early-middle summer varied widely at depths < 150
207 m (Figure 3b). In contrast, those values showed less variability in late summer and were highest
208 near the surface (up to 0.022 nm^{-1} ; Figure 3b and d). At depths > 150 m, all S_{CDOM} values

209 approached $0.0167 \pm 0.0005 \text{ nm}^{-1}$ with increasing depth (dotted rectangle in Figure 3d).

210 For surface waters, our results thus showed that $a_{\text{CDOM}}(440)$ values decreased in association with
211 increases in S_{CDOM} from early to late summer (for up to 2.5 months). It is well known that as a
212 result of solar irradiation, high-weight molecules are transported into low-weight molecules that
213 absorb light in the shorter spectral wavelengths, a phenomenon called photo-bleaching. The spectral
214 slope therefore increases after the photo-bleaching (Twardowski and Donaghay, 2002). The
215 timescale is likely one to three months (Granskog et al., 2009). Satellite-derived sea ice
216 concentration images further showed that surface waters at most of our sampling stations were ice-
217 free and therefore exposed to solar irradiation (Figure 2). All these results demonstrate photo-
218 bleaching occurred during our observations.

219 For deep waters, CDOM absorption properties were stable (Figure 3a and b). Because CDOM in
220 these waters is considered to be biologically unavailable or refractory, those absorption values can
221 be considered as an end-member for refractory CDOM. If so, the proportion of CDOM lability
222 could be optically quantified when the other end-member from labile CDOM is obtained. Further
223 work is necessary to examine this issue.

224

225 **3.2. Relationship between CDOM and hydrography**

226 Because salinity can be a good proxy of Arctic Ocean hydrography (e.g., Carmack et al., 1989;
227 Macdonald et al., 1989; Matsuoka et al., 2012), relationships between CDOM absorption properties
228 (i.e., $a_{\text{CDOM}}(440)$ and S_{CDOM}) and salinity were examined (Figure 4). At salinity < 28 , two types of
229 waters were distinguished: 1) river waters with a strong negative correlation between $a_{\text{CDOM}}(440)$
230 and salinity and 2) ice-melt waters showing both low $a_{\text{CDOM}}(440)$ and salinity (Figure 4a; see also
231 Matsuoka et al., 2012). These waters were observed in the Mackenzie shelf-basin area in the late
232 summer (black circles: MALINA cruise); river waters samples were collected in the Mackenzie
233 River mouth, while ice melt waters samples were taken near the sea ice, far away from the river
234 mouth ($> 300 \text{ km}$). Data points at salinities < 28 located in the Chukchi-Beaufort Seas in mid-

235 summer (red diamonds: ICESCAPE 2011 cruise) were not far away from the negative $a_{\text{CDOM}(440)}$
236 versus salinity relationship for MALINA cruise (Figures 4a and b). In this salinity range, S_{CDOM}
237 exhibited low variability (0.0196 ± 0.0011 ; Figure 4b), which is consistent with the value reported
238 by Matsuoka et al. (2012) (0.0192 ± 0.0011).

239 At salinities > 28 , $a_{\text{CDOM}(440)}$ values for the MALINA cruise tended to be lower than those for
240 the ICESCAPE 2010&2011 cruises (early-middle summer) conducted in the Chukchi-Beaufort Seas
241 (Figure 4c). This was especially true in the surface layer (i.e., $28 < \text{salinity} < 30.7$), where the lower
242 $a_{\text{CDOM}(440)}$ values for the MALINA cruise corresponded to slightly but significantly higher S_{CDOM}
243 values (0.0189 ± 0.0006) compared to those for the ICESCAPE 2010&2011 cruises ($0.0182 \pm$
244 0.0004 and 0.0183 ± 0.0012 , respectively) (T-test, $p < 0.0001$; Figure 4c and d), which suggests
245 that photo-bleaching occurred from early-middle to late summer (Nelson et al., 1998; Twardowski
246 and Donaghay, 2002, Matsuoka et al., 2011; see also Figure 3). In other words, CDOM in the
247 Chukchi-Beaufort Seas observed during the early-middle summer cruises might have been
248 relatively *new* because of *in situ* production and/or input from the Bering Sea (Matsuoka et al.,
249 2011; Shen et al., 2012).

250 The negative relationship between $a_{\text{CDOM}(440)}$ and salinity in the Lower Halocline Water (LHW:
251 $33.9 < \text{salinity} < 34.7$) and Atlantic Layer (AL: salinity > 34.7 ; our water samples were always
252 collected at depths shallower than 850 m) was very similar among cruises (Figure 4c). This
253 relationship was likely stable across ice-free seasons and areas of the WAO. So the $a_{\text{CDOM}(440)}$
254 versus salinity relationship could be specific to these waters.

255 In the intermediate layer between the surface and the LHW+AL layers (i.e., $30.7 < \text{salinity} <$
256 33.9), $a_{\text{CDOM}(440)}$ values for the ICESCAPE 2010&2011 cruise in the Chukchi-Beaufort Seas were
257 significantly higher than those for MALINA in the Mackenzie shelf-basin area (T-test, $p < 0.0001$).
258 Correspondingly, S_{CDOM} values in the intermediate layer were much lower for the ICESCAPE
259 2010&2011 cruises than for the MALINA cruise (T-test, $p < 0.0001$; Figure 4d). Based on field
260 observations, Nelson et al. (1998) suggested that bacteria produce CDOM when taking up dissolved
10

261 organic carbon (DOC), which is also consistent with results from laboratory experiments. Moran et
262 al. (2000), Helms et al. (2008), and Ortega-Retuerta et al. (2009) observed that heterotrophic
263 bacterial activity is associated with a decrease in the spectral slope of CDOM absorption over time.
264 Note, however, that this result is contrary to the one obtained by Nelson et al., 2004. This contrast
265 might originate from differences in substrate of organic matter utilized by bacteria and/or in distinct
266 bacterial assemblages. Considering these findings, we hypothesized that the significantly low S_{CDOM}
267 values observed in this study are associated with heterotrophic microbial activity.

268 To test this hypothesis, a vertical section of CDOM absorption properties, as well as salinity and
269 phaeopigments in the intermediate layer (i.e., $30.7 < \text{salinity} < 33.9$), along the transect from the
270 Kotzebue Sound (KS) to the Chukchi Hotspot (CH) was further analyzed (Figure 5). The transect
271 covered both river-influenced and biologically productive areas sampled during the ICESCAPE
272 2010 cruise (see Figure 1 for location). Waters showing high $a_{\text{CDOM}(440)}$ and low salinity values
273 were observed in the surface layer of the KS, indicating river-influenced waters (Figure 5a and b).
274 Further offshore, this trend was no longer observed in the surface layer of the CH. Relatively high
275 $a_{\text{CDOM}(440)}$ values, corresponding to significantly low S_{CDOM} values, were observed near the bottom
276 of the CH. Interestingly, the low S_{CDOM} values were associated with high concentrations of
277 phaeopigments ($r^2 = 0.70$, $p < 0.0001$; Figure 5c and d); BP measurements are not shown here
278 because of the limited number of data points along this transect. Because phaeopigments reflect
279 degradation products of phytoplankton intermediated by bacteria, this result partly supports our
280 hypothesis that both the high $a_{\text{CDOM}(440)}$ and low S_{CDOM} values observed in this study resulted from
281 heterotrophic microbial activity.

282

283 **3.3. Relationship between the spectral slope of CDOM absorption and bacteria**

284 To examine the direct relationship between the spectral slope of CDOM absorption and bacteria,
285 S_{CDOM} was regressed against BP and BA (Figure 6; chl *a* concentrations, temperature and nitrate
286 concentrations were also regressed against S_{CDOM}). There was a weak but significant negative

287 correlation between BP and S_{CDOM} (Figure 6a; $r^2 = 0.20$, $p < 0.0001$). The coefficient of
288 determination for this relationship was the second highest following the BP versus chl *a* relationship
289 ($r^2 = 0.24$, $p < 0.0001$; Table 1). Temperature showed the third highest correlation with slightly
290 lower coefficient of determination ($r^2 = 0.18$, $p < 0.0001$). Significant correlations were not found
291 for BP versus salinity or nitrate concentrations.

292 S_{CDOM} was negatively correlated with BA (Figure 6b; $r^2 = 0.26$, $p < 0.0001$). The coefficient of
293 determination for this relationship was the highest, followed by BA versus chl *a* ($r^2 = 0.22$, $p <$
294 0.0001 ; Table 1). Similarly to BP, temperature showed the third highest correlation with BA ($r^2 =$
295 0.17 , $p < 0.0001$). No significant correlations were found between BA and either salinity or NO_3
296 concentration. These results suggest that low S_{CDOM} values were generally associated with high BP
297 and BA in our environments.

298 A similar regression analysis was performed for the spectral parameters $S_{275-295}$, $S_{350-400}$, and S_R ,
299 as done by Helms et al. (2008). Although results using $S_{350-400}$ were similar to those using S_{CDOM}
300 (Table 2), none of them revealed higher correlations with BP and BA than S_{CDOM} ; S_{CDOM} is a better
301 variable to reflect bacterial activity.

302

303 3.4. Multiple relationships among variables

304 To examine relationships among several variables, a PCA analysis was performed. The extracted
305 axes of the PCA (Figure 7) can be interpreted as follows. Principal Component 1 (PC1) made the
306 largest contribution, explaining 30.9 % of total variance. The positive component was strongly
307 related to chl *a*, $a_{CDOM}(440)$, BA, and BP and had a weak relationship with temperature and salinity.
308 Thus, the positive PC1 was considered to reflect production of organic matter. More interestingly,
309 S_{CDOM} alone showed the opposite trend compared to the above-mentioned variables (i.e., production
310 of organic matter), suggesting that negative PC1 might reflect the decomposition of organic matter.

311 Principal Component 2 (PC2) explained 21.4 % of total variance. The negative component was
312 strongly related to NO_3 concentration and apparent oxygen utilization (AOU) and was weakly

313 related to salinity. NO_3 and AOU were tightly correlated, consistent with recent findings by
314 Matsuoka et al. (2012) for these two variables in the salinity range of 30.7-33.9 (or approximately
315 50-200 m depth; see their Figures 3c and d). Thus, negative PC2 was considered to reflect the
316 aphotic zone. In contrast, the positive PC2 might reflect the euphotic zone, which is further
317 supported by the fact that this component was weak but related to the production of organic matter.

318 Note that result of salinity in the PCA analysis is not surprising and can be explained as follows.
319 First, salinity exhibited an opposite trend compared to that shown by S_{CDOM} . This general trend is
320 shown in Figure 4. Second, this variable had a negative direction in PC2. This result is consistent
321 with our discussion that negative PC2 represents the aphotic zone, showing higher salinity.
322 Furthermore, Figure 7 provides important information: Because only S_{CDOM} showed opposite
323 direction compared to parameters related to production of organic matter, this variable might be
324 considered to reflect the degradation products of organic matter.

325 As expected, S_{CDOM} was negatively correlated with BP and BA (Figure 6), which is consistent
326 with the result of simple regression analysis (Figure 6 and Table 1). Similarly, S_{CDOM} was negatively
327 correlated with chl *a* and phaeopigments ($p < 0.0001$ for both). By taking into account the findings
328 in Figures 5-7, our results suggest that variations in S_{CDOM} reflect the degradation of phytoplankton
329 that is associated with heterotrophic bacterial activity.

330

331 **4. Conclusions**

332 This study demonstrated that variations in the spectral slope of CDOM absorption (S_{CDOM}) are
333 partly explained by bacterial production (BP) and bacterial abundance (BA) variations. A simple
334 regression analysis showed that S_{CDOM} was related to both BA and BP, which was further supported
335 by PCA analysis. Bacterial abundance and production is likely dependent on bioavailability of
336 DOM (e.g., Moran et al., 2000; Helms et al., 2008; Ortega-Retuerta et al., 2009). The spectral slope
337 of CDOM reflects to some extent the level of DOC availability (Moran et al., 2000; Helms et al.,
338 2008; Ortega-Retuerta et al., 2009). Therefore, it is consistent that S_{CDOM} is significantly correlated

339 with bacterial activity. Further work is necessary to better understand changes in CDOM cycling in
340 the Arctic Ocean.

341

342 **Acknowledgements**

343 We are grateful to the captain and crews of the Canadian Icebreaker *CCGS Amundsen* and the
344 US icebreaker *USCGC Healy*. CTD deployment and data processing were made by Y. Gratton, L.
345 Prieur, and C. Marec for MALINA and J. Swift and R. S. Pickart for ICESCAPE cruises. Water
346 samples from a small boat were provided by S. B. Hooker. Fluorometric chlorophyll *a*
347 concentrations were measured by S. Bélanger and A. Mignot for MALINA and K. R. Arrigo, M.
348 Mills, G. van Dijken, Z. Brown, M. Palmer, and K. Lowry for ICESCAPE cruises. Nitrate
349 concentrations were provided by J. E. Tremblay, P. Raimbault, N. Garcia, and J. Gagnon for
350 MALINA and S. Becker for ICESCAPE cruises. Technical supports by Q. Allison, S. Tolley, S.
351 Hiller, S. Laney, and S. Roberts are much appreciated. Bacterial abundance and production data
352 during MALINA were kindly provided by D. Marie, F. Joux and W.H. Jeffrey. Comments from two
353 anonymous reviewers greatly improved the manuscript. This study was conducted as part of the
354 MALINA Scientific Program funded by ANR (Agence nationale de la recherche), INSU-CNRS
355 (Institut national des sciences de l'univers – Centre national de la recherche scientifique), CNES
356 (Centre national d'études spatiales) and ESA (European Space Agency). This research was also
357 supported by the Ocean Biology and Biogeochemistry Program and the Cryosphere Science
358 Program of the National Aeronautic and Space Administration (NNX10AF42G to K. Arrigo). We
359 also thank a joint contribution to the research programs of UMI Takuvik, ArcticNet (Network
360 Centres of Excellence of Canada) and the Canada Excellence Research Chair in Remote Sensing of
361 Canada's New Arctic Frontier.

362

363 **References**

364 Armstrong, F.A. Stearns, J., C. R., and Strickland, J. D. H., 1967, The measurement of upwelling

- 365 and subsequent biological processes by means of the Technicon AutoAnalyzer™ and
366 associated equipment. *Deep-Sea Res.* 14(3): 381-389.
- 367 Arrigo, K. R., Perovich, D.K., Pickart, R.S., Brown, Z.W., van Dijken, G.L., Lowry, K.E., Mills,
368 M.M., Palmer, M.A., Balch, W.M., Bahr, F., Bates, N.R., Benitez-Nelson, C., Bowler, B.,
369 Brownlee, E., Ehn, J.K., Frey, K.E., Garley, R., Laney, S.R., Lubelczyk, L., Mathis, J.,
370 Matsuoka, A., Mitchell, B.G., Moore, G.W.K., Ortega-Retuerta, E., Pal, S., Polashenski,
371 C.M., Reynolds, R.A., Schieber, B., Sosik, H.M., Stephens, M., and Swift, J.H., 2012,
372 Massive Phytoplankton Blooms Under Arctic Sea Ice, *Science*, 10.1126/science.1215065.
- 373 Azam, F., Fenchel, T., Field, J.G., Gray, J.S., Meyer-Rei, L.A., and Thingstad F., 1983, The
374 Ecological Role of Water-Column Microbes in the Sea, *Mar. Ecol. Prog. Ser.*, 10, 257-263.
- 375 Babin, M., Stramski, D., Ferrari, G. M., Claustre, H., Bricaud, A., Obolensky, G., and Hoepffner,
376 N., 2003, Variations in the light absorption coefficients of phytoplankton, nonalgal particles,
377 and dissolved organic matter in coastal waters around Europe, *J. Geophys. Res.*, 108,
378 doi:10.1029/2001JC00082.
- 379 Bussmann, I., 1999, Bacterial utilization of humic substances from the Arctic Ocean, *Aquat. Microb.*
380 *Ecol.*, 19, 37-45.
- 381 Carmack, E.C., Macdonald, R.W., and Papadakis, J.E., 1989, Water mass structure and boundaries
382 in the Mackenzie shelf estuary, *J. Geophys. Res.*, 94, 18043–18055.
- 383 Carder, K.L., Steward, R.G., Harvey, G.R., and Ortner, P.B., 1989, Marine humic and fulvic
384 acids: Their effects on remote sensing of ocean chlorophyll, *Limnol. Oceanogr.*, 34, 68–81.
- 385 Carpenter, J.H., 1965, The accuracy of the Winkler method for dissolved oxygen, *Limnol.*
386 *Oceanogr.*, 10, 135-140.
- 387 Culberson, C.H., 1991, Dissolved Oxygen, WHP Operations and Methods, Unpublished manuscript,
388 15 pp.
- 389 Ducklow, H.W., 1992, Factors regulating bottom-up control of bacterial biomass in open ocean
390 plankton communities, *Ergeb. Limnol.*, 37, 207–217.

- 391 Garneau, M.-E., Roy S., Lovejoy, C., Gratton, Y., and Vincent W.F., 2008, Seasonal dynamics of
392 bacterial biomass and production in a coastal arctic ecosystem: Franklin Bay, western
393 Canadian Arctic, *J. Geophys. Res.*, 113, C07S91, doi:10.1029/2007JC004281.
- 394 Gasol, J.M., Zweifel, U.L., Peters, F., Fuhrman, J.A., Hagstrom, A., 1999, Significance of size and
395 nucleic acid content heterogeneity as measured by flow cytometry in natural planktonic
396 bacteria. *Appl. Environ. Microbiol.* 65, 4475-4483.
- 397 Guéguen, C. McLaughlin, F. A., Carmack, E. C., Itoh, M. Narita, H., and Nishino, S., 2012, The
398 nature of colored dissolved organic matter in the southern Canada Basin and East Siberian
399 Sea, *Deep-Sea Res., II*, 81-84, 102-113.
- 400 Granskog, M., Macdonald, R. W., Kuzyk, Z. Z. A., Senneville, S., Mundy, C.-J., Barber, D., Stern,
401 G. A., and Saucier, F., 2009, Coastal conduit in southwestern Hudson Bay (Canada) in
402 summer: Rapid transit of freshwater and significant loss of colored dissolved organic matter,
403 *J. Geophys. Res.*, 114, C08012, doi:10.1029/2009JC005270.
- 404 Grasshoff, K., Kremling, K. and Ehrhardt, M. (Eds.), 1999, *Methods of seawater analysis*, New
405 York, Wiley-VCH.
- 406 Helms, J.R., Stubbins, A., Ritchie, J.D., Minor, E.C., Kieber, D. J., and Mopper, K., 2008,
407 Absorption spectral slopes and slope ratios as indicators of molecular weight, sources, and
408 photobleaching of chromophoric dissolved organic matter, *Limnol. Oceanogr.*, 53, 955–
409 969.
- 410 Holm-Hansen, O., Lorenzen, C.J., Holmes, R.W., and Strickland, J.D.H., 1965, Fluorometric
411 Determination of Chlorophyll, *J. Cons. perm. int. Explor. Mer.*, 30, 3-15.
- 412 Kirchman, D.L., Moran, X.A.G., and Ducklow, H., 2009, Microbial growth in the polar oceans –
413 role of temperature and potential impact of climate change, *Nature Rev.*, 7, 451-459.
- 414 Kirchman, D.L., 1993, Leucine incorporation as a measure of biomass production by heterotrophic
415 bacteria, in: PF, K. (Ed.), *Handbook of methods in aquatic microbial ecology*. Lewis
416 Publishers, Boca Raton, pp. 509-512.

- 417 Legendre, P., and Legendre, L., 1998, Numerical Ecology, New York.
- 418 Marie, D., Partensky, F., Jacquet, S., Vaulot, D., 1997, Enumeration and cell cycle analysis of
419 natural populations of marine picoplankton by flow cytometry using the nucleic acid stain
420 SYBR Green I. *Appl. Environ. Microbiol.* 63, 186-193.
- 421 Matsuoka, A., Bricaud, A., Benner, R., Para, J., Sempere, R., Prieur, L., Bélanger, S., and Babin, M.,
422 2012, Tracing the transport of colored dissolved organic matter in water masses of the
423 Southern Beaufort Sea: relationship with hydrographic characteristics, *Biogeosciences*, 9,
424 doi: 10.5194/bg-9-925-2012.
- 425 Matsuoka, A., Hill, V., Huot, Y., Bricaud, A., and Babin, M., 2011, Seasonal variability in the light
426 absorption properties of western Arctic waters: parameterization of the individual
427 components of absorption for ocean color applications, *J. Geophys. Res.*, 116,
428 doi:10.1029/2009JC005594.
- 429 Matsuoka, A., Hooker, S.B., Bricaud, A., Gentili, B., and Babin, M., 2013, Estimating absorption
430 coefficients of colored dissolved organic matter (CDOM) using a semi-analytical algorithm
431 for southern Beaufort Sea waters: applications to deriving concentrations of dissolved
432 organic carbon from space, *Biogeosciences*, 10, doi: 10.5194/bg-10-917-2013.
- 433 Matsuoka, A., Babin, M., Doxaran, D., Hooker, S.B., Mitchell, B.G., Bélanger, S., and Bricaud, A.,
434 2014, A synthesis of light absorption properties of the Arctic Ocean: application to semi-
435 analytical estimates of dissolved organic carbon concentrations from space, *Biogeosci.*, 11,
436 3131-3147, doi:10.5194/bg-11-3131-2014.
- 437 Macdonald, R.W., Carmack, E.C., McLaughlin, F.A., Iseki, K., Macdonald, D.M., and O'Brien,
438 M.C., 1989, Composition and modification of water masses in the Mackenzie shelf estuary,
439 *J. Geophys. Res.*, 94, 18057–18070.
- 440 McClelland, J.W., Déry, S.J., Peterson, B.J., Holmes, R.M., and Wood, E.F., 2006, A pan-arctic
441 evaluation of changes in river discharge during the latter half of the 20th century, *Geophys.*
442 *Res. Lett.*, 33, L06715, doi:10.1029/2006GL025753.

- 443 Moran, M.A., Sheldon, W. M. Jr., and Zepp, R. G., 2000, Carbon loss and optical property changes
444 during long-term photochemical and biological degradation of estuarine dissolved organic
445 matter, *Limnol. Oceanogr.*, 45(6), 1254-1264.
- 446 Miller, W.L., Moran, M.A., Sheldon, W.M., Zepp, R.G., and Opsahl, S., 2002, Determination of
447 apparent quantum yield spectra for the formation of biologically labile photoproducts,
448 *Limnol. Oceanogr.*, 47, 343–352.
- 449 Nelson, N.B., Siegel, D.A., Michaels, A.F., 1998, Seasonal dynamics of colored dissolved
450 material in the Sargasso Sea, *Deep Sea Research Part 1*, 45, 931-957.
- 451 Nelson, N. B., Carlson, C. A., and Steinberg, D. K., 2004, Production of chromophoric dissolved
452 organic matter by Sargasso Sea microbes, *Mar. Chem.*, 89, 273-287.
- 453 Nelson, N.B., Siegel, D.A., Carlson, C.A., Swan, C., Smethie, W.M. Jr., and Khatiwala, S., 2007,
454 Hydrography of chromophoric dissolved organic matter in the North Atlantic, *Deep Sea*
455 *Research Part 1*, 54, 710-731.
- 456 Ortega-Retuerta, E., Jeffrey, W.H., Babin, M., Bélanger, S., Benner, R., Marie, D., Matsuoka, A.,
457 Raimbault, P., and Joux, F., 2012, Carbon fluxes in the Canadian Arctic: patterns and
458 drivers of bacterial abundance. Production and respiration on the Beaufort Sea margin, *Bio*
459 *geosci.*, 9, 3679-3692.
- 460 Ortega-Retuerta, E., Frazer, T.K., Duarte, C.M., Ruiz-Halpern, S., Tovar-Sanchez, A., Arrieta, J.M.,
461 and Reche, I., 2009, Biogeneration of chromophoric dissolved organic matter by bacteria
462 and krill in the Southern Ocean, *Limnol. Oceanogr.*, 54(6), 1941-1950.
- 463 Peterson, B.J., Holmes, R.M., McClelland, J.W., Vorosmarty, C.J., Lammers, R.B., Shiklomanov,
464 A.I., Shiklomanov, I.A., and Rahmstorf, S., 2002, Increasing river discharge to the Arctic
465 Ocean, *Science*, 298, 2171-2173.
- 466 Raymond, P.A., McClelland, J.W., Holmes, R.M., Zhulidov, A.V., Mull, K., Peterson, B.J., Striegl,
467 R.G., Aiken, G.R., and Gurtovaya T.Y., 2007, Flux and age of dissolved organic carbon
468 exported to the Arctic Ocean: A carbon isotopic study of the five largest arctic rivers,

- 469 Global. *Biogeochem. Cycles.*, 21, GB4011, doi:10.1029/2007GB002934.
- 470 Shen, Y., Fichot, C.G., and Benner, R., 2012, Dissolved organic matter composition and
471 bioavailability reflect ecosystem productivity in the Western Arctic Ocean, *Biogeosci.*, 9,
472 4993-5005.
- 473 Smith, D.C., Azam, F., 1992, A simple, economical method for measuring bacterial protein
474 synthesis rates in seawater using 3H-leucine. *Mar Microb Food Webs* 6, 107-114.
- 475 Suzuki, K.W., Kasai, A., Nakayama, K., and Tanaka, M., 2012, Year-round accumulation of
476 particulate organic matter in the estuarine turbidity maximum: comparative observations in
477 three macrotidal estuaries (Chikugo, Midori, and Kuma Rivers), southwestern Japan, *J.*
478 *Oceanogr.*, 68, 453-471.
- 479 Twardowski, M.S., and Donaghay, P.L., 2002, Photobleaching of aquatic dissolved materials:
480 Absorption removal, spectral alteration, and their interrelationship, *J. Geophys. Res.*,
481 107(C8), 3091, 10.1029/1999JC000281.
- 482 Uitz, J., Huot, Y., Bruyant, F., Babin, M., and Claustre, H., 2008, Relating phytoplankton
483 photophysiological properties to community structure on large scales, *Limnol. Oceanogr.*,
484 53(2), 614-630.
- 485 Yamashita, Y., Nosaka, Y., Suzuki, K., Ogawa, H., Takahashi, K., and Saito, H., 2013,
486 Photobleaching as a factor controlling spectral characteristics of chromophoric dissolved
487 organic matter in open ocean, *Biogeosci.*, 10, 7207-7217, doi:10.5194/bg-10-7207-2013.
488

489 **Figure captions**

490 Figure 1. Locations of sampling stations for ICESCAPE 2010 (blue crosses), ICESCAPE 2011 (red
 491 diamonds), and MALINA (black circles) cruises in the Arctic Ocean. A transect from
 492 Kotzebue Sound (KS) to the Chukchi Hotspot (CH) is shown as a black line. Vertical
 493 sections of CDOM absorption properties as well as salinity and phaeopigment
 494 concentrations along this transect in the intermediate layer (i.e., $30.7 < \text{salinity} < 33.9$) are
 495 shown in Figure 5.

496 Figure 2. Mean sea ice concentration images provided by the using satellite microwave sensor,
 497 DMSP SSM/I, during (a) MALINA, (b) ICESCAPE2010, and (c) ICESCAPE2011 cruises.
 498 These images were generated by averaging daily images available during each cruise.
 499 Sampling stations are also displayed with white circles, yellow crosses, and red diamonds,
 500 respectively.

501 Figure 3. Vertical profiles of (a) CDOM absorption coefficients at 440 nm ($a_{\text{CDOM}(440)}$, m^{-1}) and (b)
 502 their spectral slope (S_{CDOM} , nm^{-1}). X-axis for (a) is log-transformed to show variability in
 503 both low and high $a_{\text{CDOM}(440)}$ values. Mean profiles of (c) $a_{\text{CDOM}(440)}$ and (d) S_{CDOM} with
 504 10-m intervals. Standard deviations are shown as horizontal bars.

505 Figure 4. Upper panels: CDOM absorption coefficients at 440 nm as a function of salinity (S) for
 506 (a) the whole salinity range and (c) for $S \geq 28$. A linear fit provided by Matsuoka et al.
 507 (2012) is shown in grey. Data points along this fit correspond to river-influenced waters.
 508 Data points for ice melt waters are shown in the circle in (a). Lower panels: spectral slope of
 509 CDOM absorption coefficients, S_{CDOM} as a function of salinity for (b) the whole salinity
 510 range and (d) for $S \geq 28$.

511 Figure 5. Vertical sections of (a) salinity, CDOM absorption properties (b) $a_{\text{CDOM}(440)}$ and (c)
 512 S_{CDOM} , and (d) phaeopigment concentrations along the transect from Kotzebue Sound (KS)
 513 to the Chukchi Hotspot (CH).

514 Figure 6. Relationship between S_{CDOM} and (a) bacterial production (BP, $\mu\text{g C m}^{-3} \text{d}^{-1}$) and (b)

515 bacterial abundance (BA, cells ml⁻¹).

516 Figure 7. Biplot of principal component analysis (PCA). The important features of this plot are as
 517 follows: 1) direction of each arrow represents contribution to principal component 1 (PC1:
 518 x-axis) and 2 (PC2: y-axis) for a given variable and 2) magnitude of an arrow represents the
 519 strength of the variable to the components. For example, BP and chl *a* concentrations
 520 showed a similar direction, suggesting they are related to each other and to positive PC1.
 521 This result is consistent with the direct regression analysis (Figure 6 and Table 1). The
 522 positive PC1 reflects production of organic matter (section 3.4). Thus, BP and chl *a*
 523 concentrations can be considered as contributors to the production of organic matter. See
 524 section 3.4 for details.

525
 526 Table 1. Summary of the Model II regression analysis for bacterial production (BP, μgC m⁻³ d⁻¹) and
 527 abundance (BA, cells ml⁻¹) as a function of chlorophyll *a* (chl *a*, mg m⁻³) concentrations, spectral
 528 slope of CDOM (S_{CDOM}, nm⁻¹), temperature (T, degrees C), salinity, and nitrate (NO₃, μmol kg⁻¹)
 529 concentrations. A total of 133 samples were used for each regression analysis.

Parameter	Statistics	Log ₁₀ (BP)	Log ₁₀ (BA)
Log ₁₀ (chl <i>a</i>)	<i>r</i> ²	0.24	0.22
	Slope	0.40	0.15
	<i>p</i> -value	< 0.0001	< 0.0001
S _{CDOM}	<i>r</i> ²	0.20	0.26
	Slope	-169.9	-73.65
	<i>p</i> -value	< 0.0001	< 0.0001
Log ₁₀ (T+2)*	<i>r</i> ²	0.18	0.17
	Slope	0.70	0.26
	<i>p</i> -value	< 0.0001	< 0.0001
Salinity	<i>r</i> ²	0.04	0.10

	Slope	0.06	0.04
	<i>p-value</i>	< 0.05	< 0.01
NO ₃	<i>r</i> ²	0.04	0.05
	Slope	-0.03	-0.01
	<i>p-value</i>	< 0.05	< 0.01

530

531 *For conversion to a base 10 logarithm, 2 was added to T.

532

533 Table 2. Determination coefficients between bacterial variables (BP or BA) and spectral slope

534 parameters (S₂₇₅₋₂₉₅, S₃₅₀₋₄₀₀, and its ratio S_R) proposed by Helms et al. (2008).

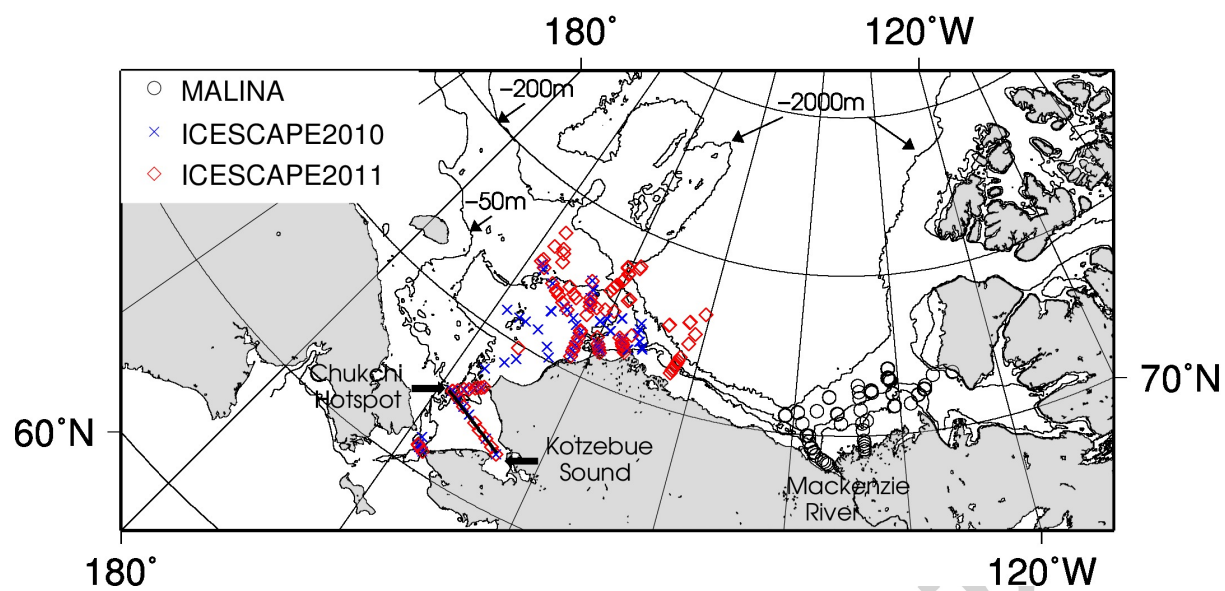
<i>r</i> ²	Log ₁₀ (BP)	Log ₁₀ (BA)
S ₂₇₅₋₂₉₅	0.11	0.12
S ₃₅₀₋₄₀₀	0.19	0.23
S _R	0.03	0.04

535

536

537

538



539

180°

120°W

540

Figure 1

541

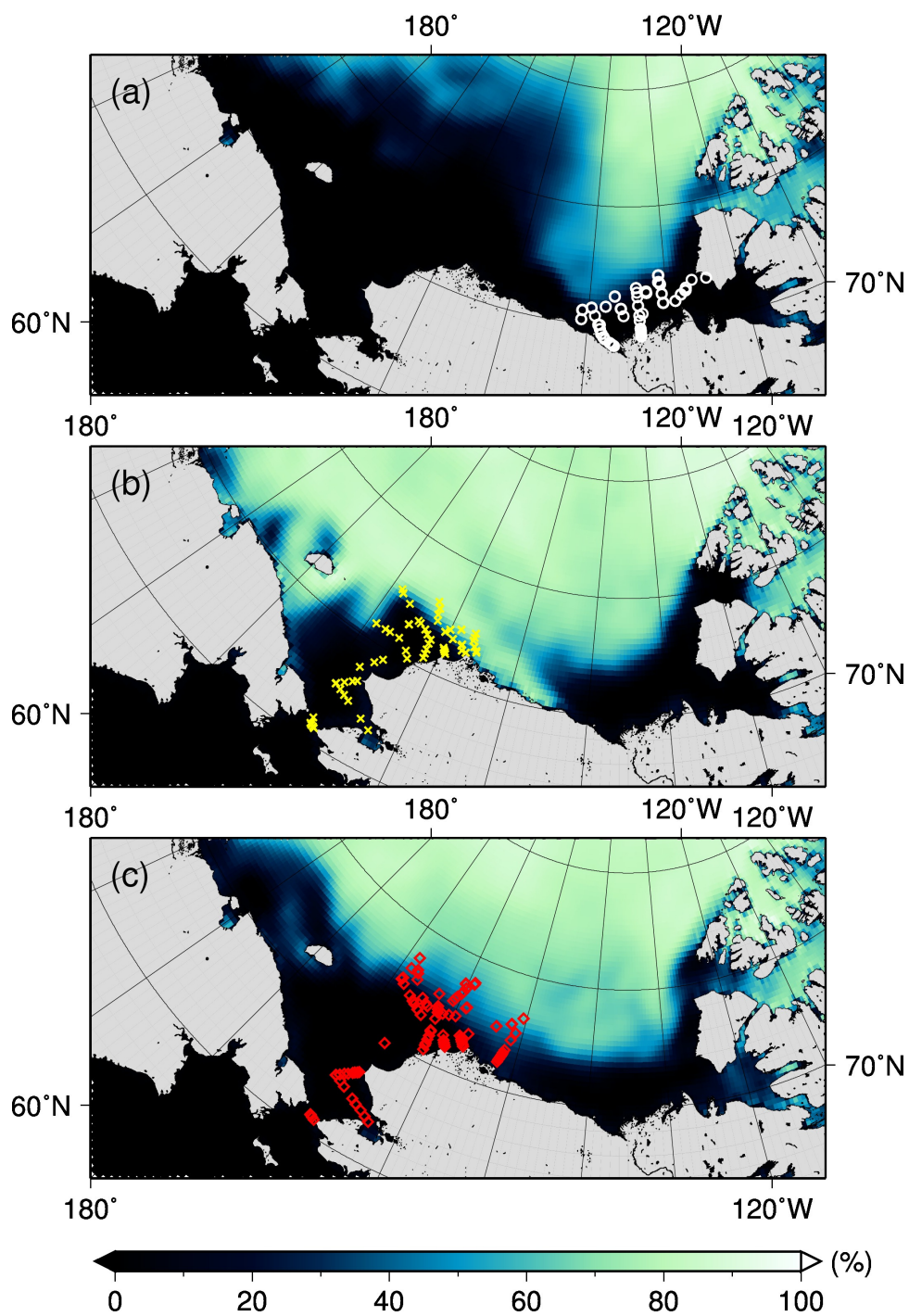
Matsuoka et al.

542

543

544

545



546

547

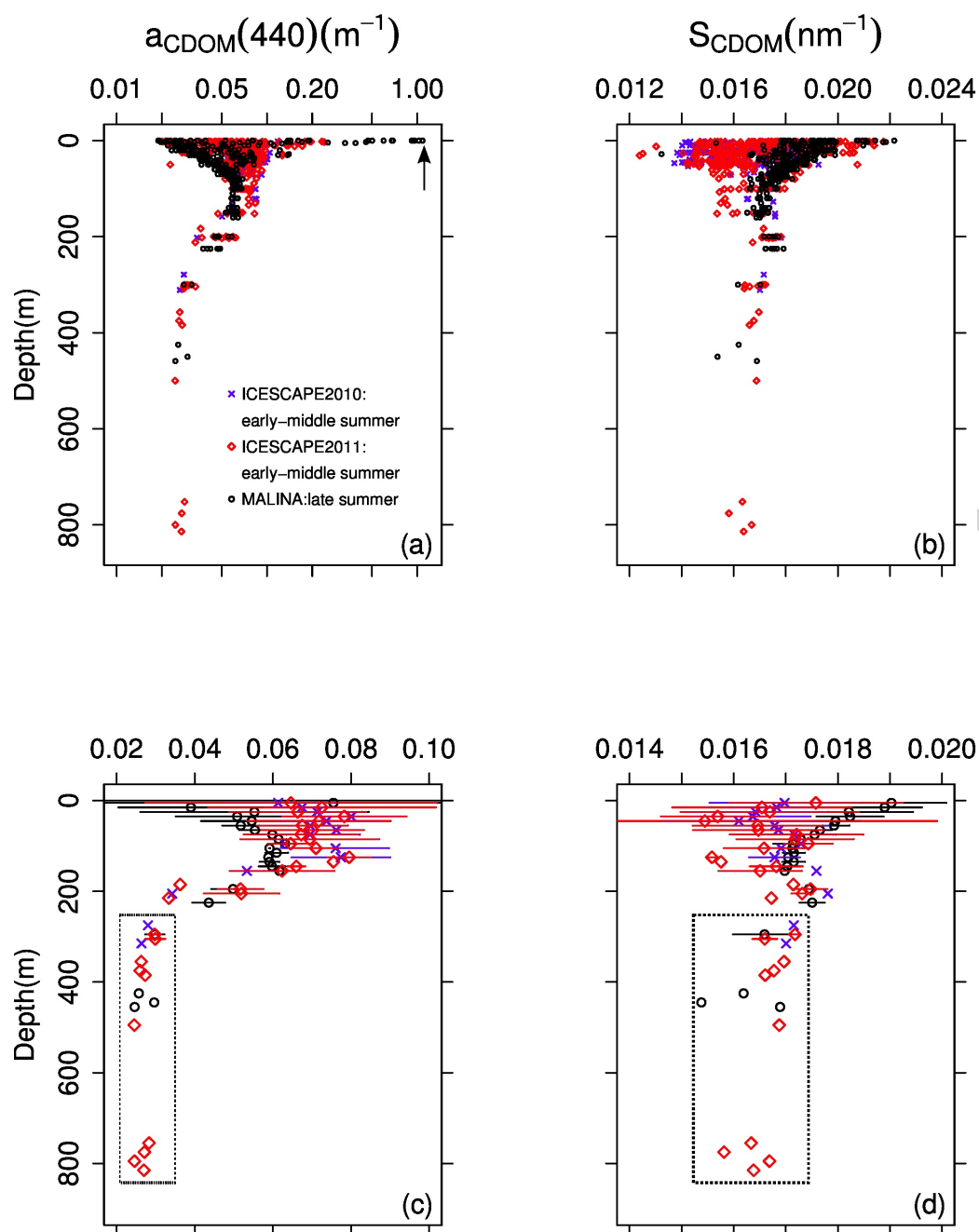
548

549

550

Figure 2

Matsuoka et al.



551

552

553

554

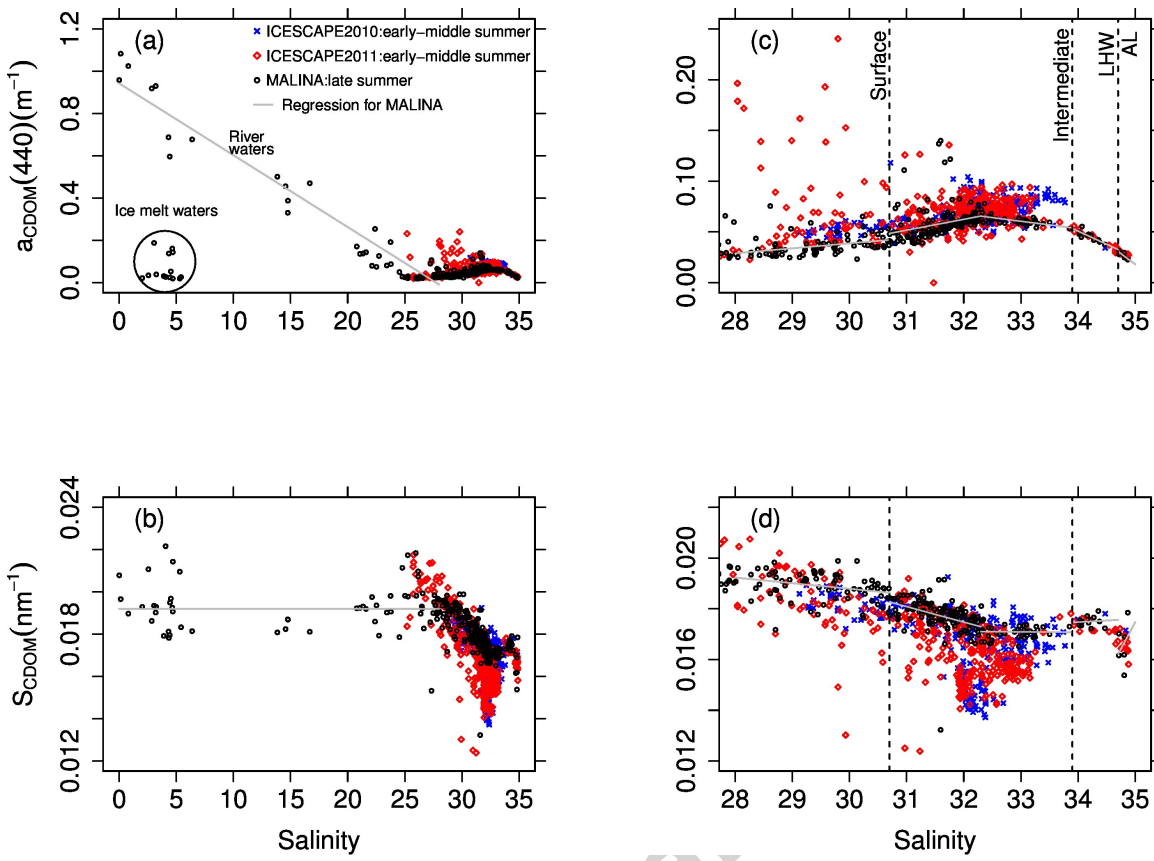
555

556

557

Figure 3

Matsuoka et al.



558

559

560

561

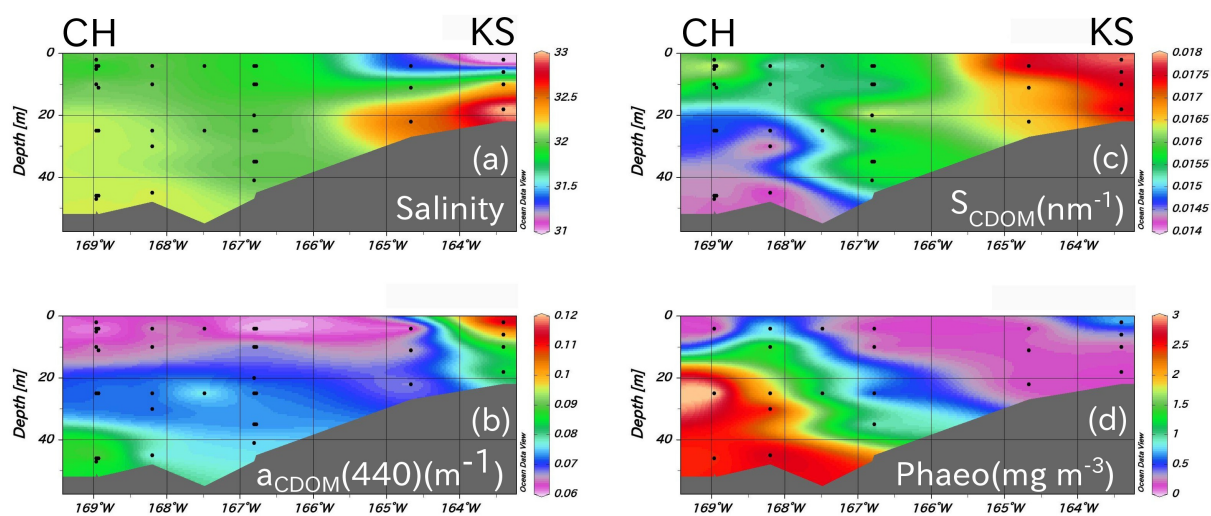
562

563

564

Figure 4

Matsuoka et al.



565

566

567

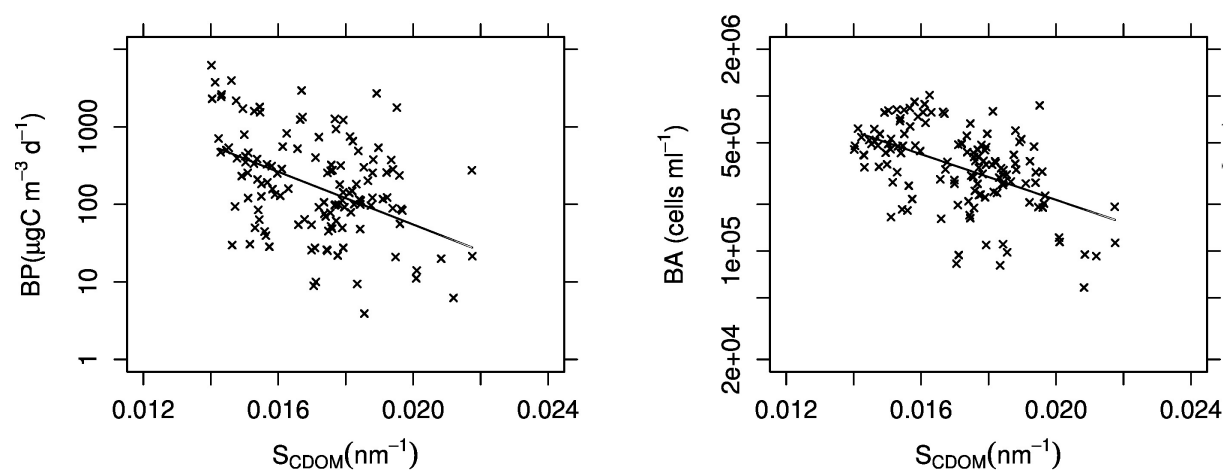
568

569

570

Figure 5

Matsuoka et al.



571

572

573

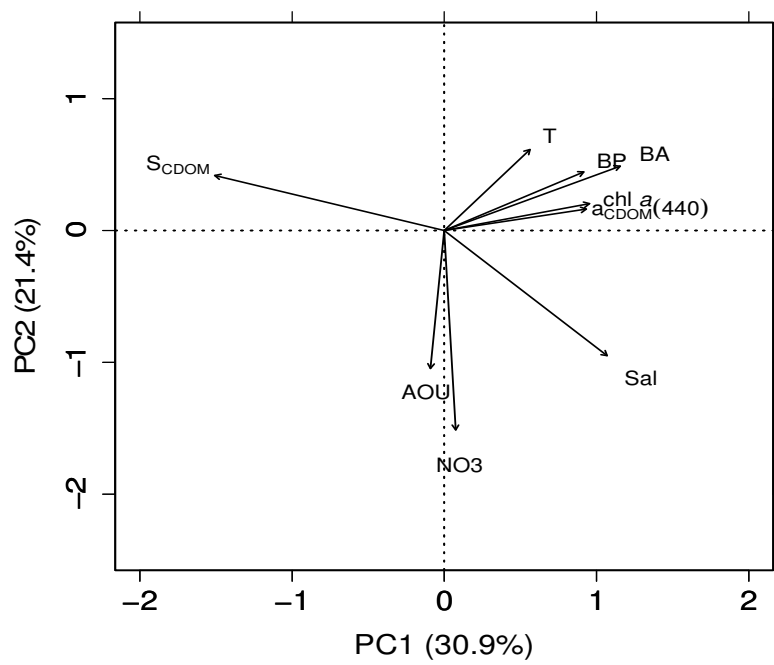
574

575

576

Figure 6

Matsuoka et al.



pt

577

578

579

580

Figure 7

Matsuoka et al.